Electronic supporting information for

Tuning the spin-transition properties of pyrene decorated 2,6-Bispyrazolylpyridine based Fe(II) complexes

Rodrigo González-Prieto,[a] Benoit Fleury,[a] Frank Schramm,[a] Giorgio Zoppellaro,[a,b] Rajadurai Chandrasekar,[a,c] Olaf Fuhr,[a] Sergei Lebedkin,[a] Manfred Kappes,[a] and Mario Ruben*[a,d]

[a] Karlsruhe Institute of Technology (KIT), Institute of Nanotechnology, Hermann-von-Helmholtz-Platz 1, 76344 Eggenstein-Leopoldshafen, Germany.[b]Department of Molecular Biosciences, University of Oslo, PO Box 1041 Blindern, Oslo NO-0316, Norway. [c]School of Chemistry, University of Hyderabad, Prof. C. R. Rao Road, Gachi Bowli, Hyderabad – 500 046, India. [d]Institut de Physique et Chimie des Matériaux de Strasbourg (IPCMS), 23 rue de Loess, BP$§, 67034 Strasbourg cedex 2, France. Fax: +49 (0) 7247 82 8976; Tel: +49 7247 82 6781; E-mail: mario.ruben@kit.edu

Table S1: Crystallographic and refinement data of **1**

Compound	**1**
Empirical formula	$C_{54}H_{34}Cl_2FeN_{10}O_8$
Formula weight	1077.66
Crystal system	monoclinic
Space group	C2/c
a/pm	1518.0(3)
b/pm	836.9(2)
c/pm	3650.5(7)
β/°	100.69(3)
$V/10^6$ pm^3	4557(2)
Z	4
μ/mm $^{-1}$	0.522
Density/g cm^{-3}	1.571
F(000)	2208
Reflections collected	6333
Independent reflections	3259 [R_{int} = 0.0484]
Indp. reflections with $F_0>4\sigma(F_0)$	2169
Restrains / parameter	0 / 408
GooF on F^2	0.932
R_1 , $wR_2[I>2\sigma(I)]$	0.0528, 0.1195
R_1 , wR_2 (all data)	0.0841, 0.1328
Largest difference peak, hole/e Å^{-3}	0.282 / –0.471

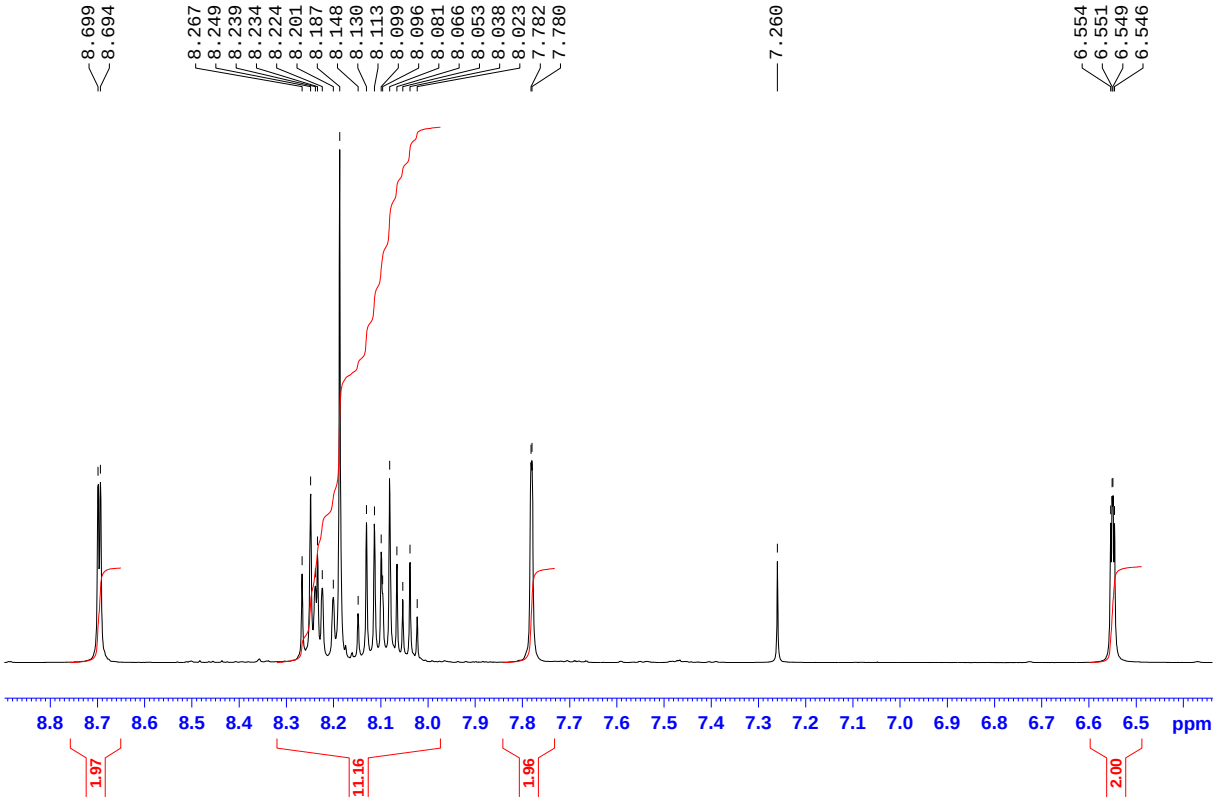

Figure S1. ^{1}H NMR spectrum of 2,6-di(1H-pyrazol-1-yl)-4-(pyren-1-yl)pyridine (**L1**) in $CDCl_3$.

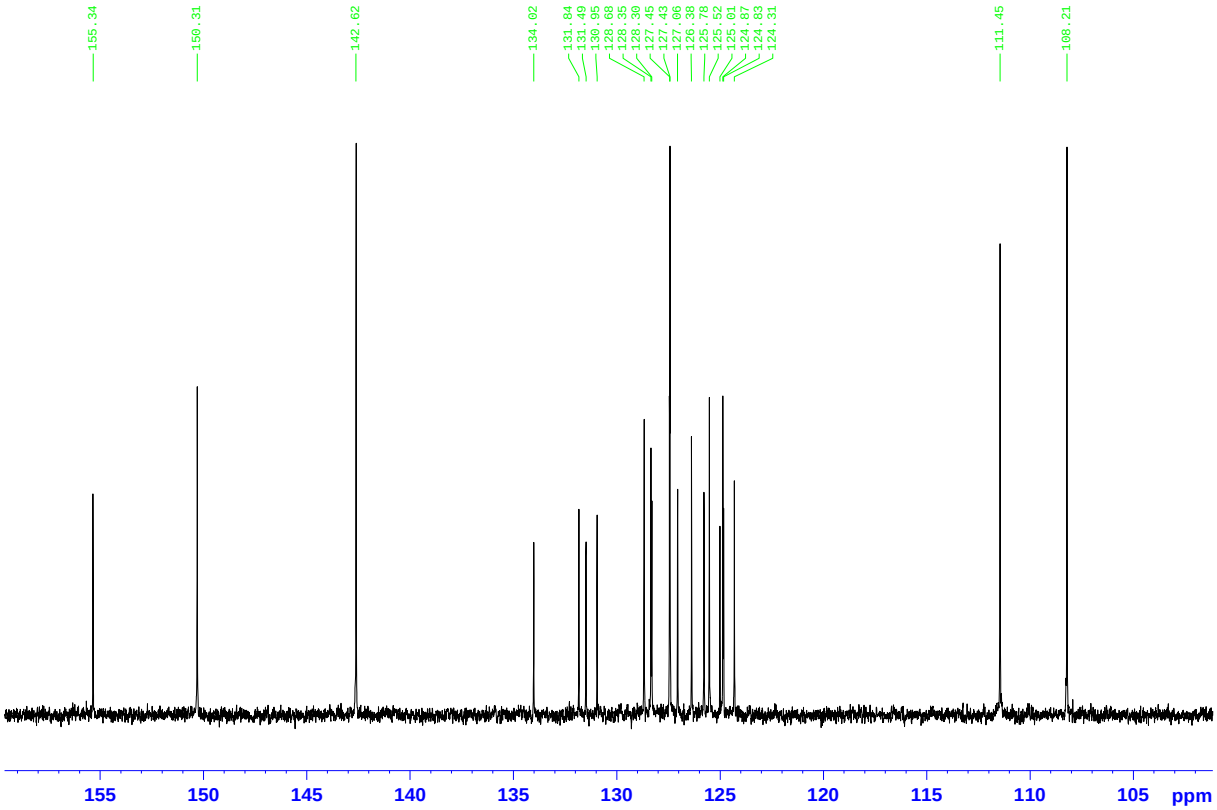

Figure S2. ^{13}C NMR spectrum of 2,6-di(1H-pyrazol-1-yl)-4-(pyren-1-yl)pyridine (**L1**) in $CDCl_3$.

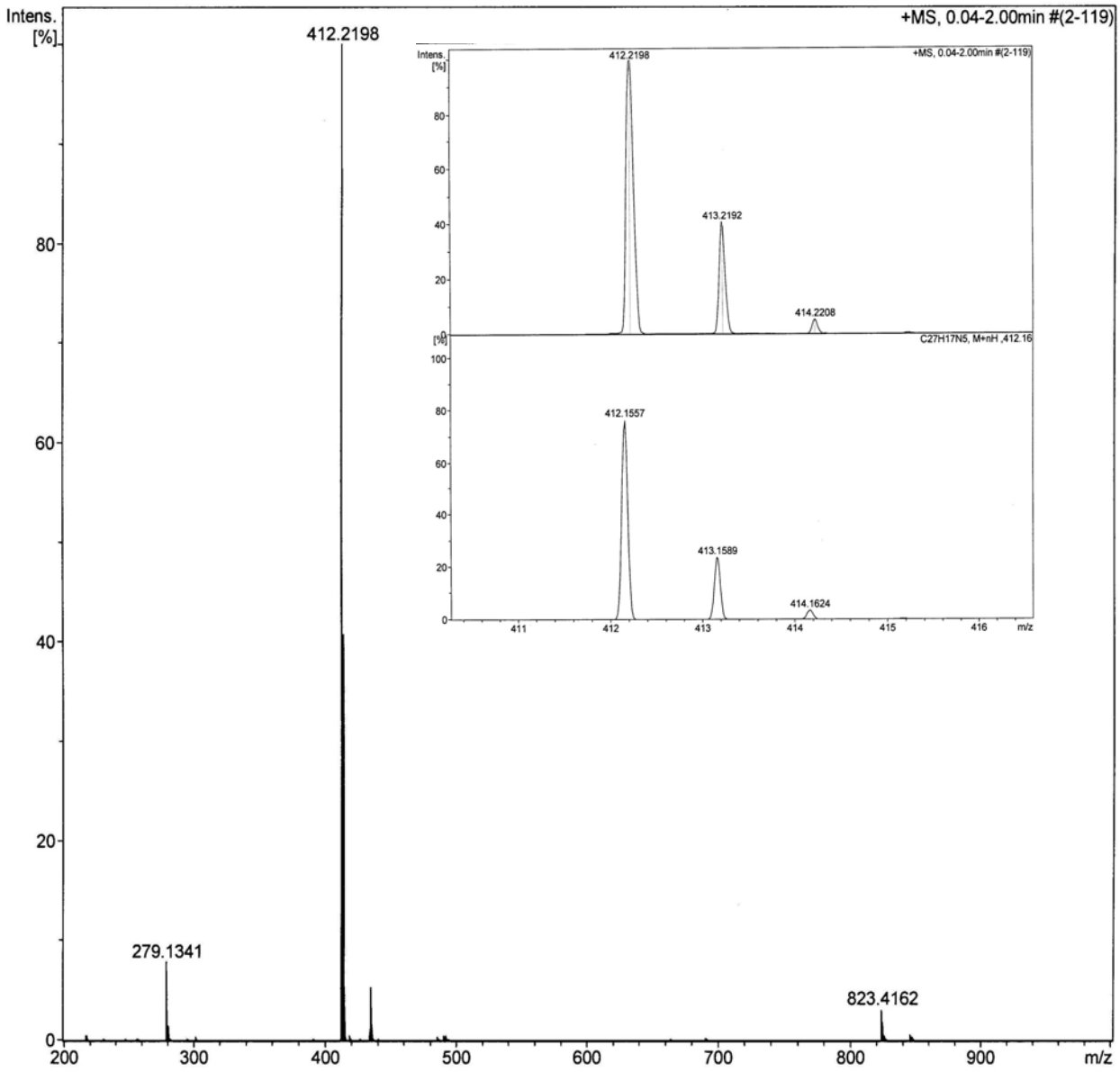

Figure S3. ESI-TOF mass spectrum of 2,6-di(1H-pyrazol-1-yl)-4-(pyren-1-yl)pyridine (**L1**). Experimental (up) and simulated (down) isotopic distributions for the most intense peak; **L1**+H^+; are shown in the inset.

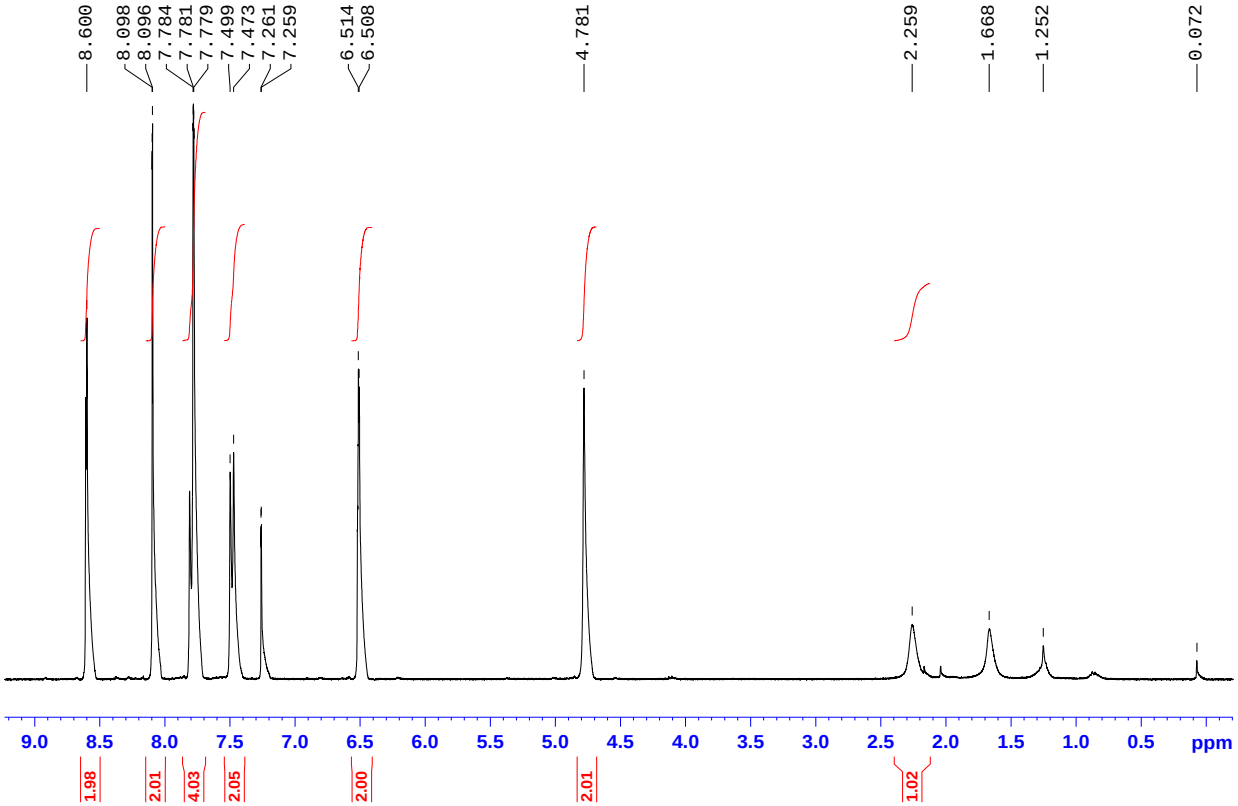

Figure S4. ^{1}H NMR spectrum of 4-(4'-hydroxymethylphenyl)-2,6-bis(pyrazol-1-yl)pyridine in $CDCl_3$.

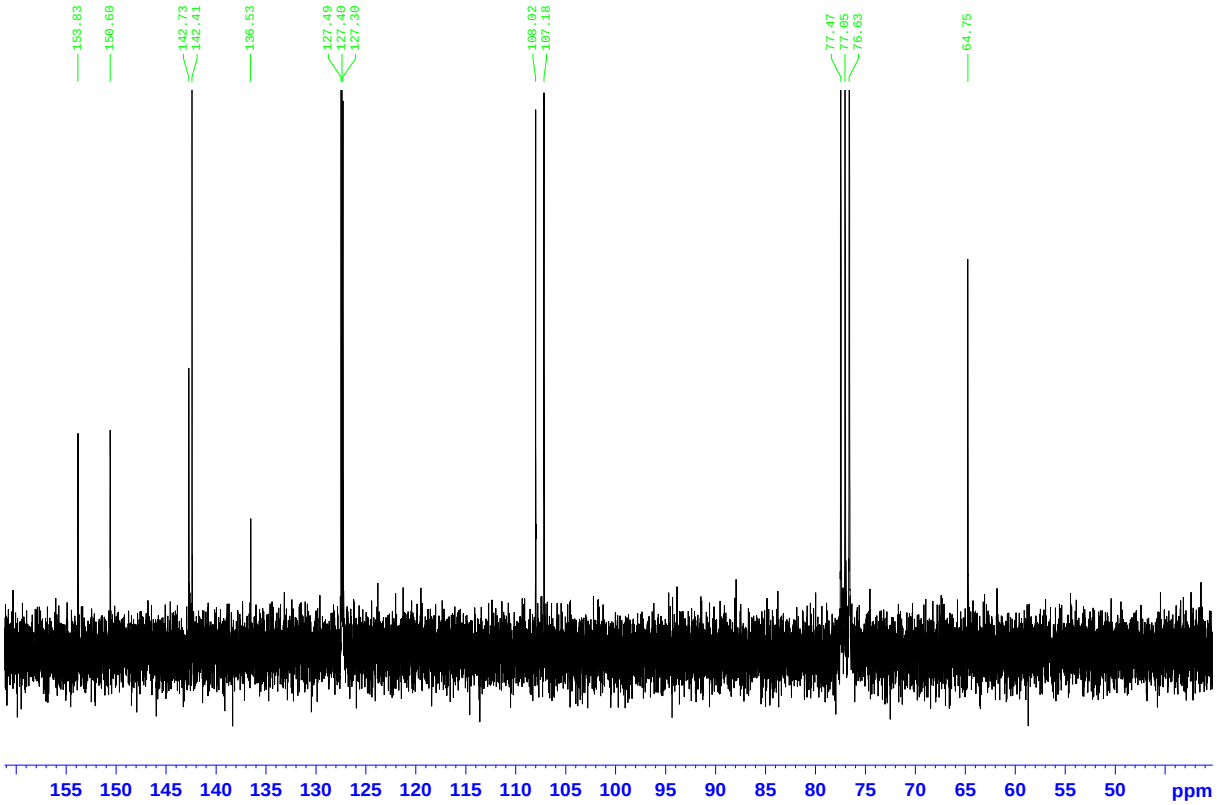

Figure S5. ^{13}C NMR spectrum of 4-(4'-hydroxymethylphenyl)-2,6-bis(pyrazol-1-yl)pyridine in $CDCl_3$.

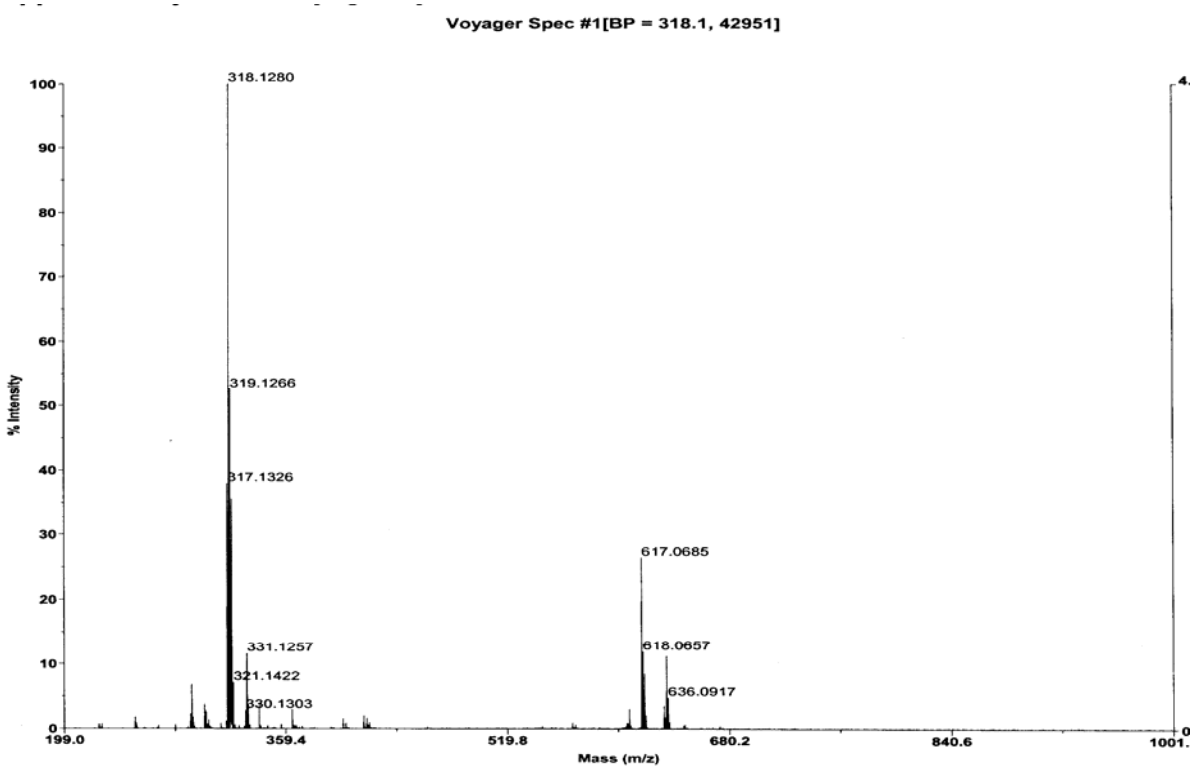

Figure S6a. MALDI mass spectrum of 4-(4'-hydroxymethylphenyl)-2,6-bis(pyrazol-1-yl)pyridine.

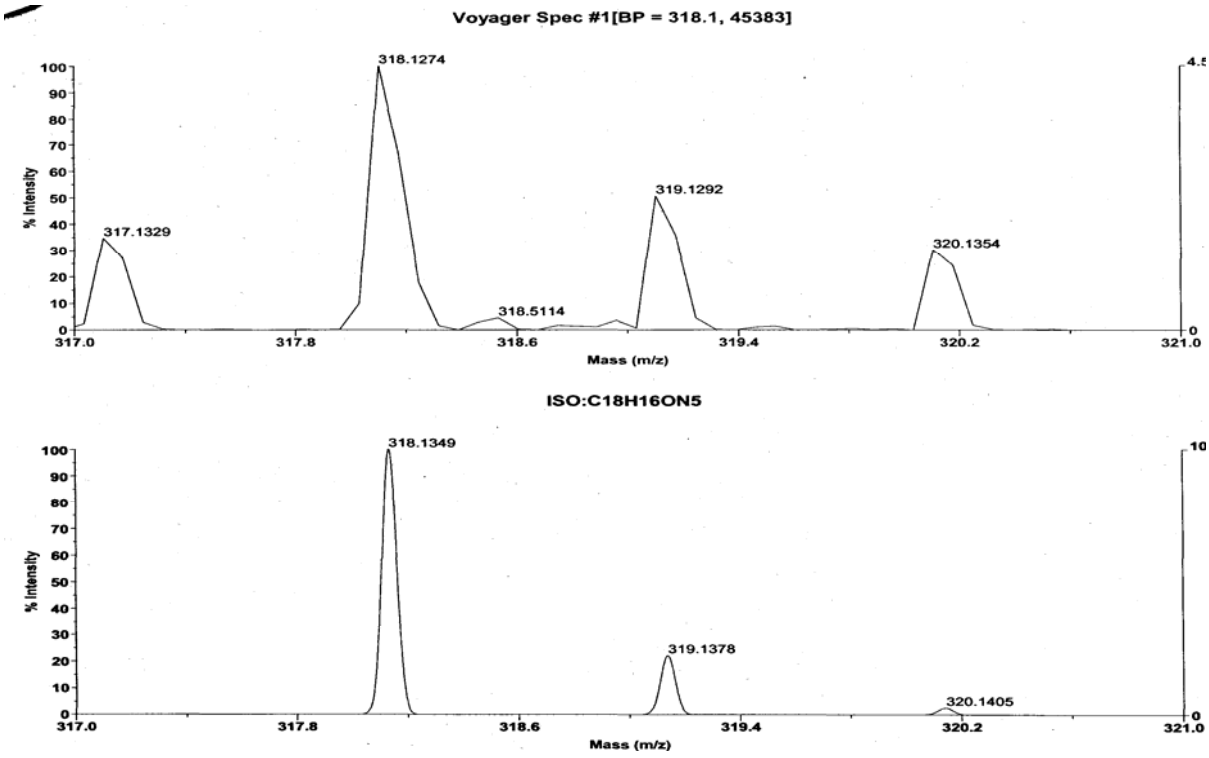

Figure S6b. Experimental (up) and simulated (down) isotopic distributions of the most intense peak; $M+H^+$.

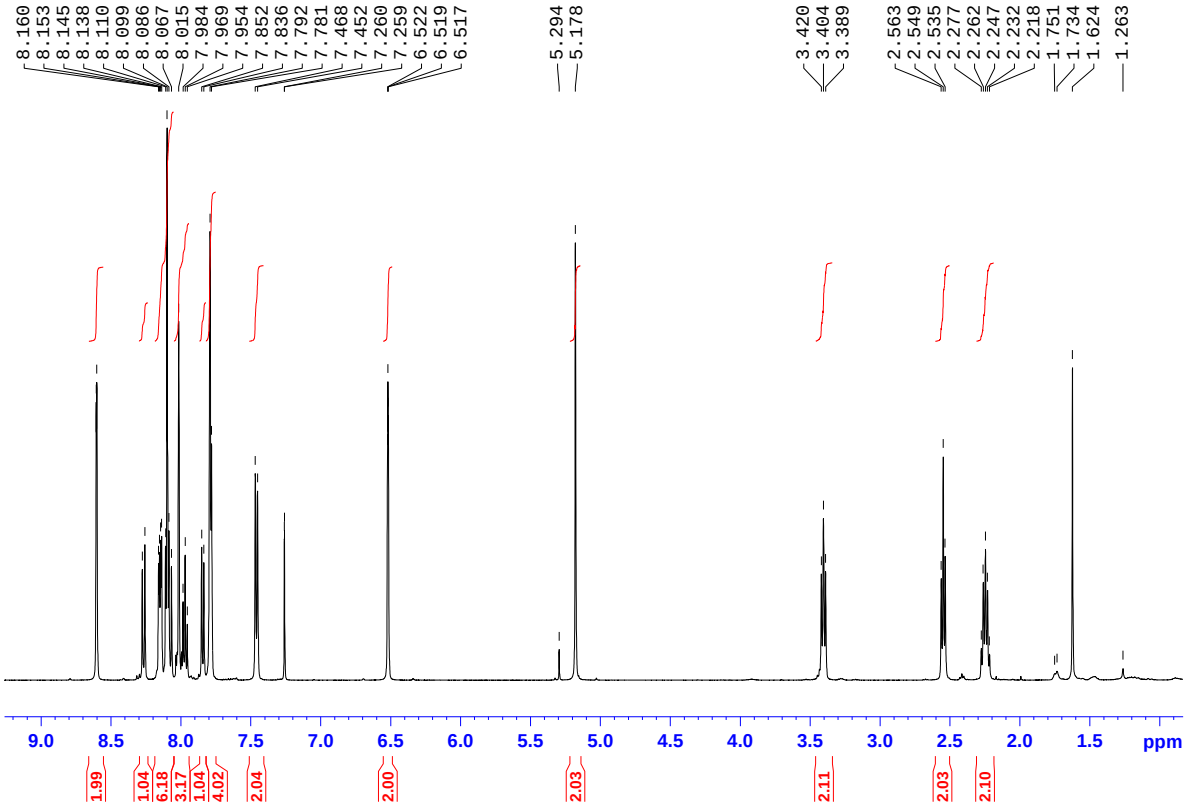

Figure S7. ^{1}H NMR spectrum of 4-(2,6-di(1H-pyrazol-1-yl)pyridin-4-yl)benzyl 4-(pyren-1-yl)butanoate (**L2**) in $CDCl_3$.

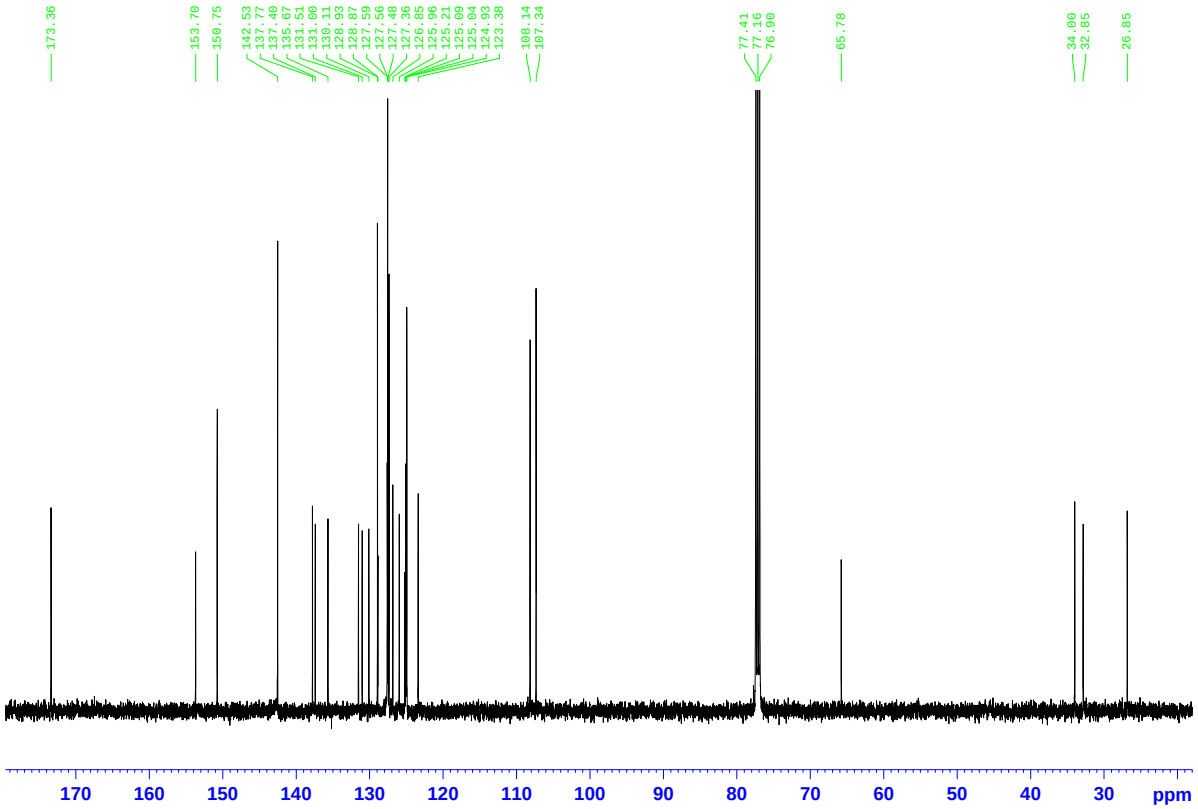

Figure S8. ^{13}C NMR spectrum of 4-(2,6-di(1H-pyrazol-1-yl)pyridin-4-yl)benzyl 4-(pyren-1-yl)butanoate (**L2**) in $CDCl_3$.

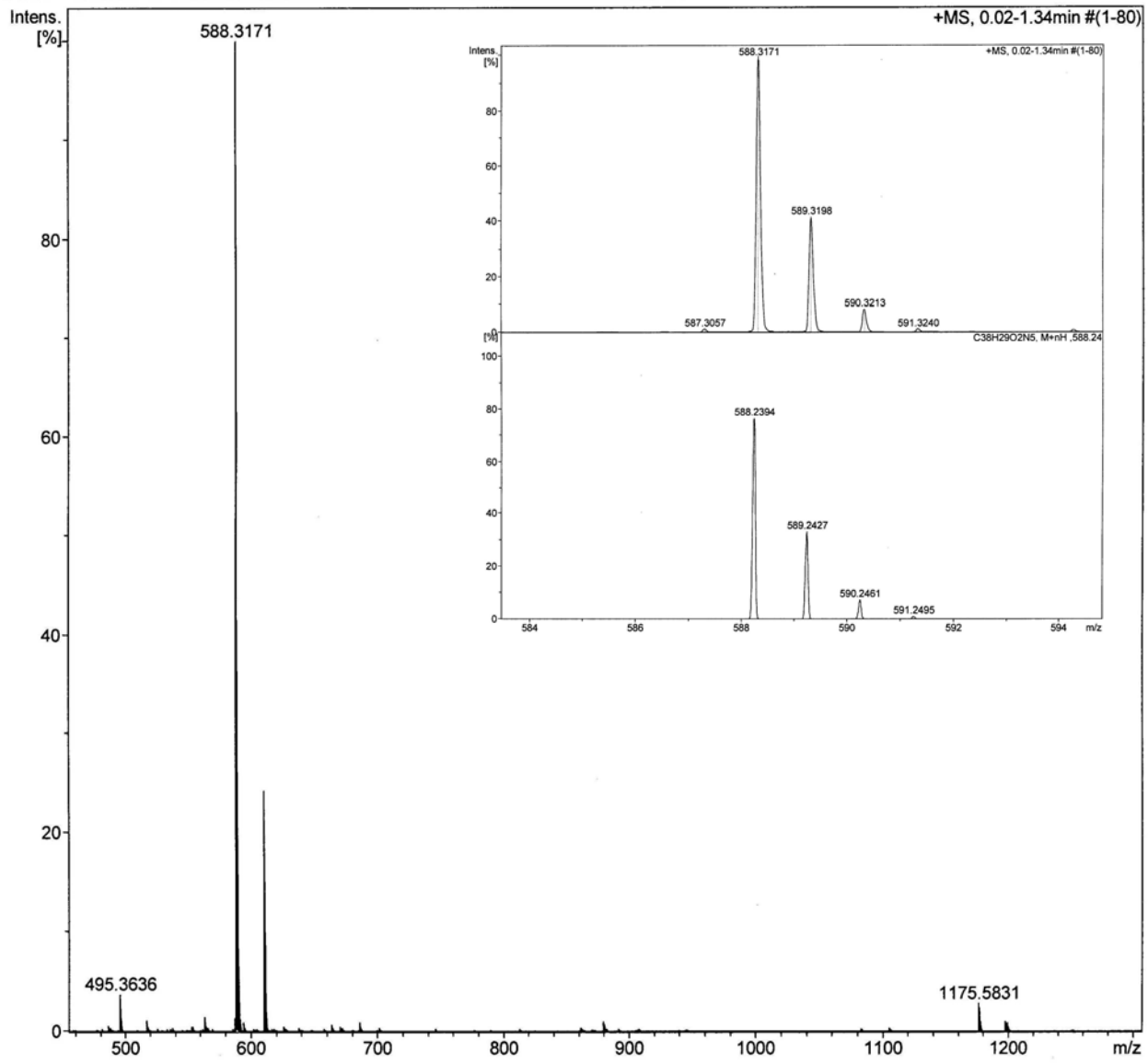

Figure S9. ESI-TOF mass spectrum of 4-(2,6-di(1H-pyrazol-1-yl)pyridin-4-yl)benzyl 4-(pyren-1-yl)butanoate (**L2**). Experimental (up) and simulated (down) isotopic distributions for the most intense peak; **L2**+H^+; are shown in the inset.

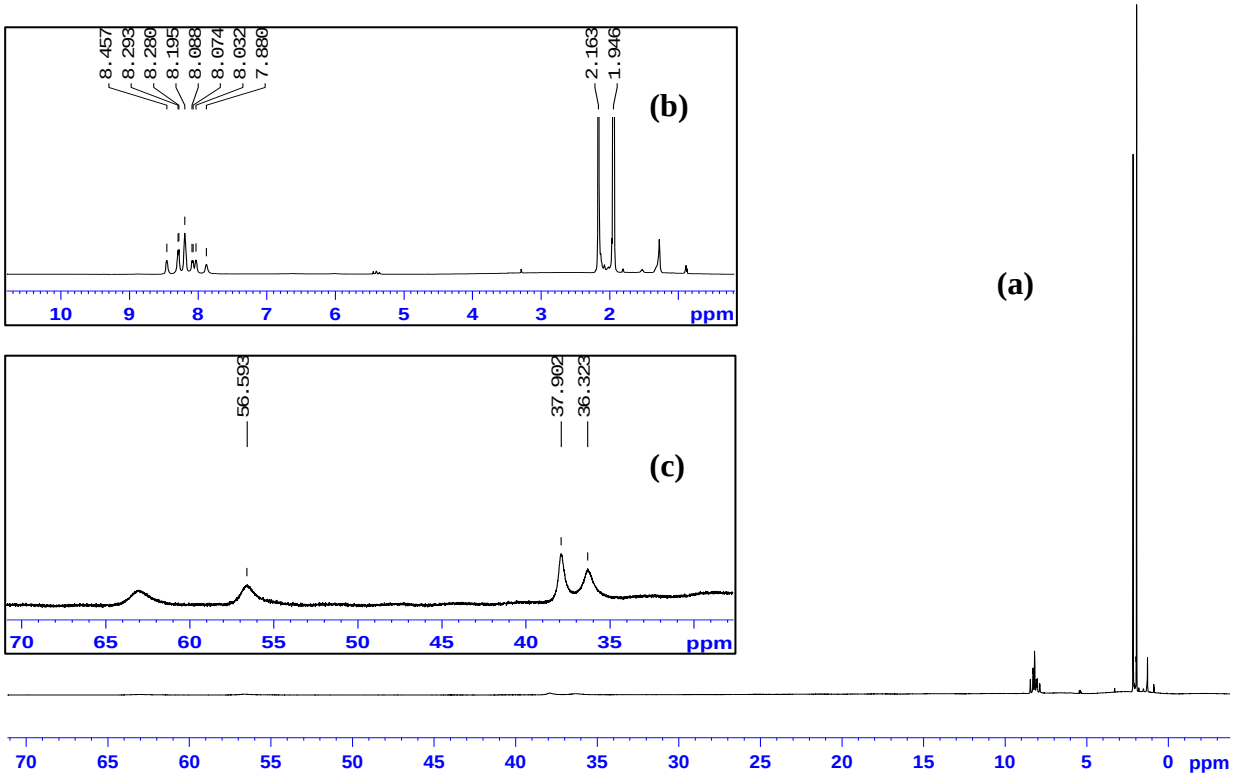

Figure S10. (**a**) ^{1}H NMR spectrum of $[Fe(L1)_2](ClO_4)_2$ (**1**) in CD_3CN. Insets (**b**) and (**c**) show enlarged zones of the whole spectrum.

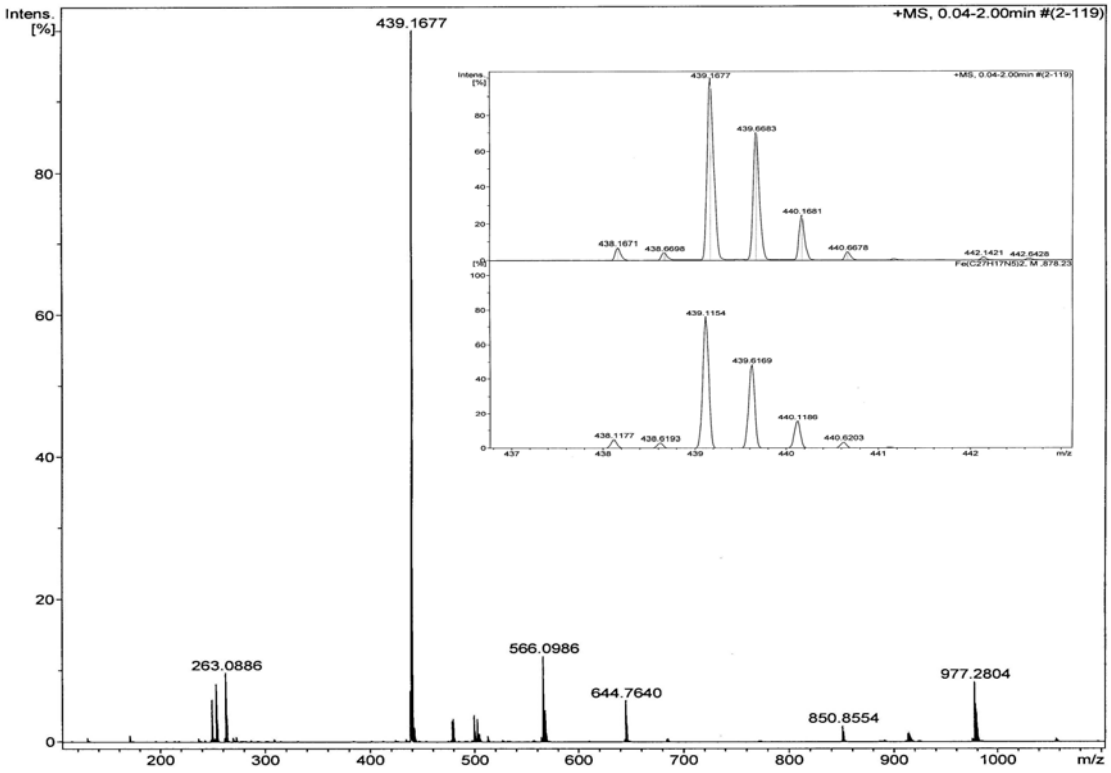

Figure S11. ESI-TOF spectrum of $[Fe(L1)_2](ClO_4)_2$ (**1**). Experimental (up) and simulated (down) isotopic distributions for the most intense peak; $\mathbf{M}^{2+}$; are shown in the inset.

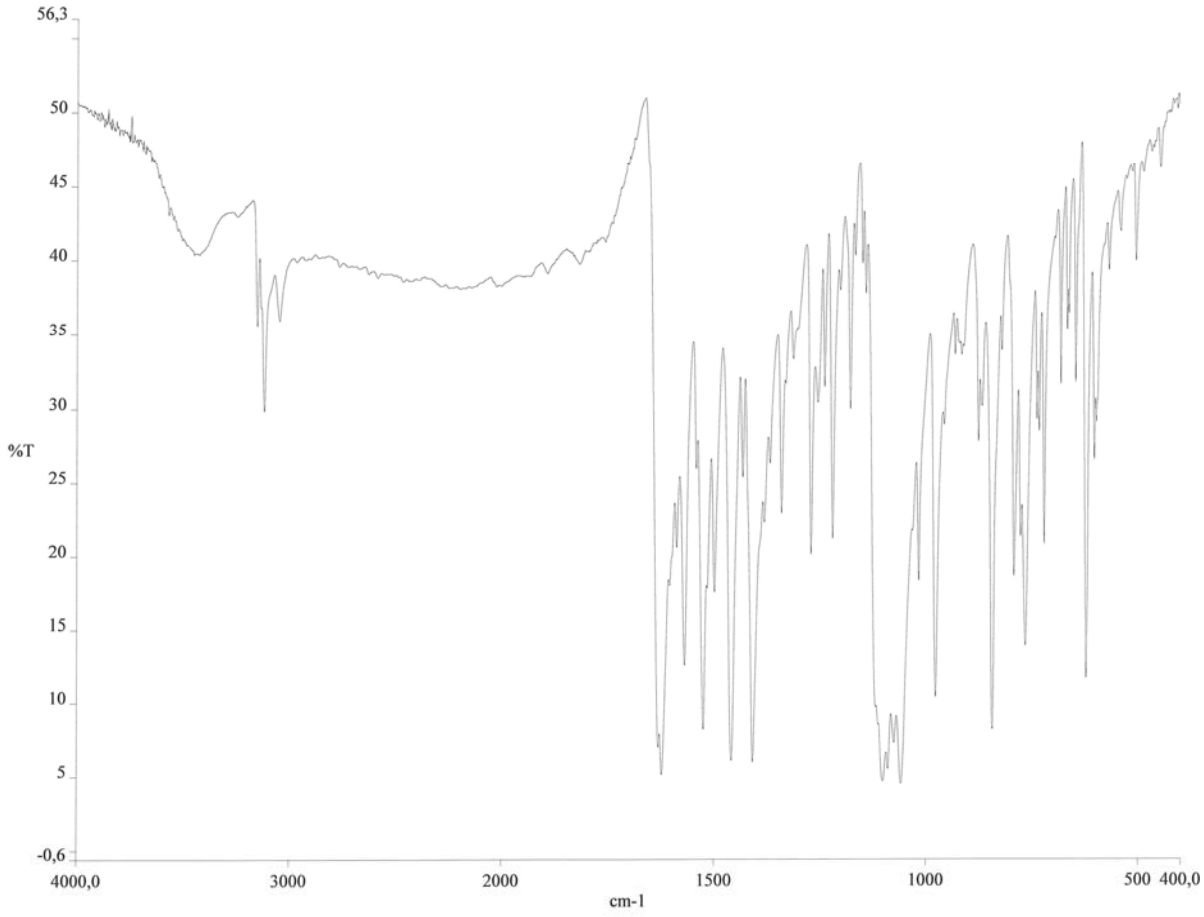

Figure S12. FT-IR spectrum of $[Fe(L1)_2](ClO_4)_2$ (**1**).

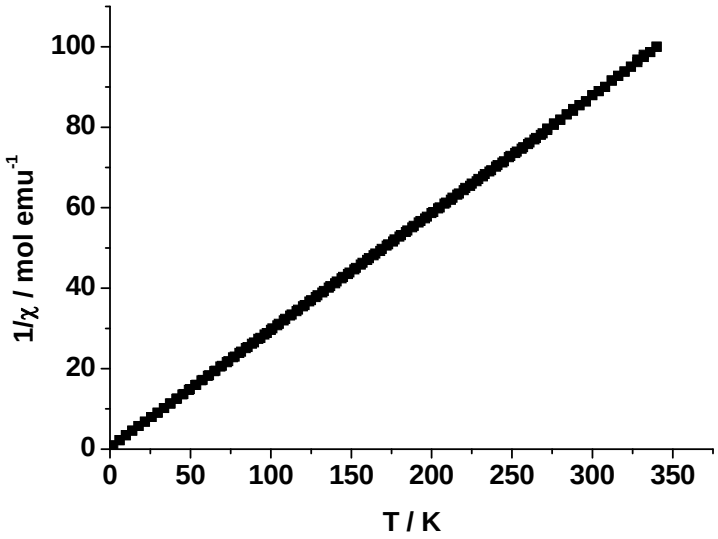

Figure S13. $1/\chi_M$ versus T plot for $[Fe(L1)_2](ClO_4)_2$ (**1**).

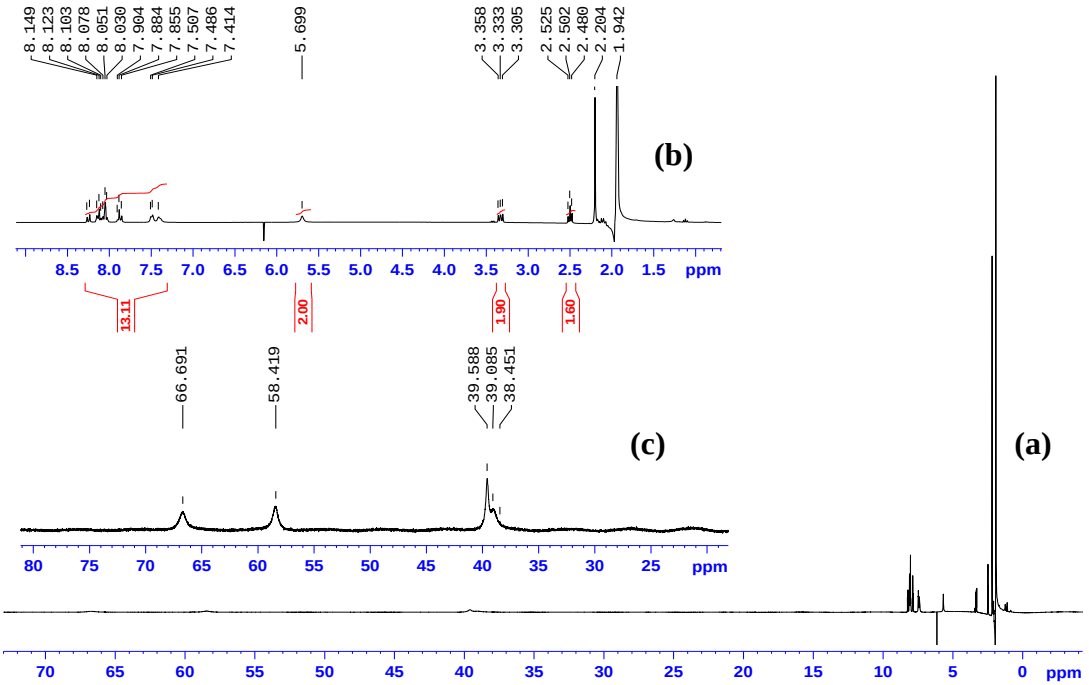

Figure S14. (**a**) ^{1}H NMR spectrum of $[Fe(L2)_2](ClO_4)_2$ (**2**) in CD_3CN. Insets (**b**) and (**c**) show enlarged zones of the whole spectrum.

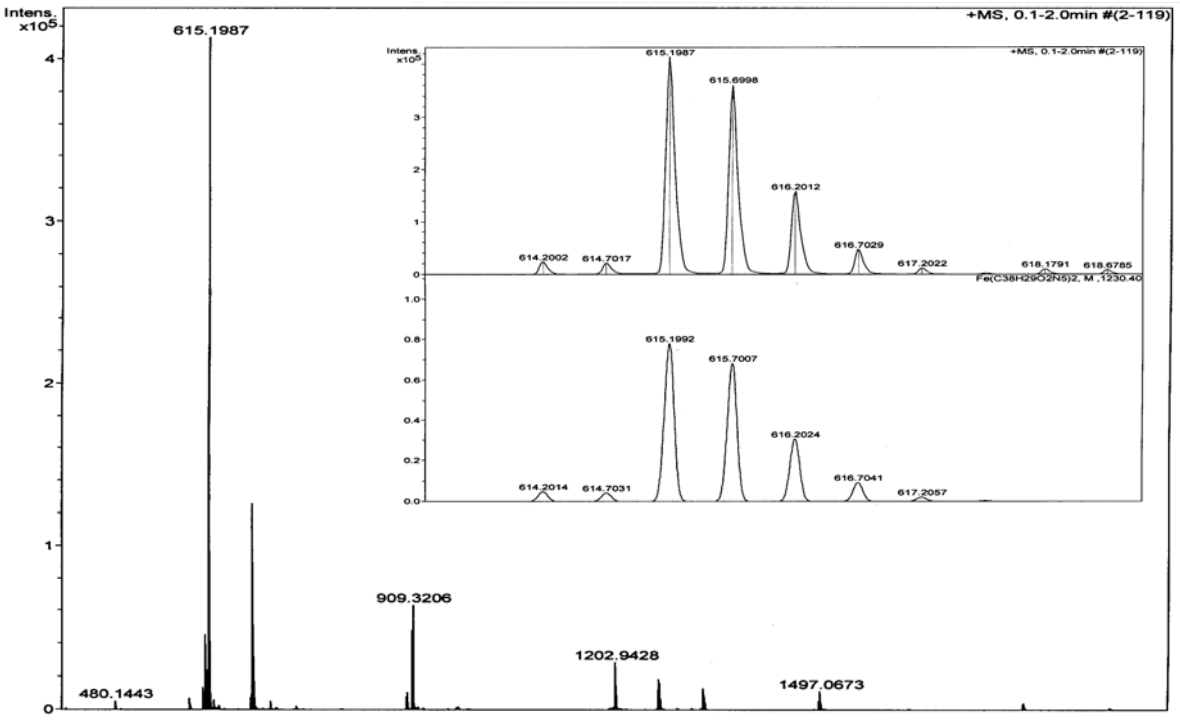

Figure S15. ESI-TOF spectrum of $[Fe(L2)_2](ClO_4)_2$ (**2**). Experimental (up) and simulated (down) isotopic distributions for the most intense peak; $\mathbf{M}^{2+}$; are shown in the inset.

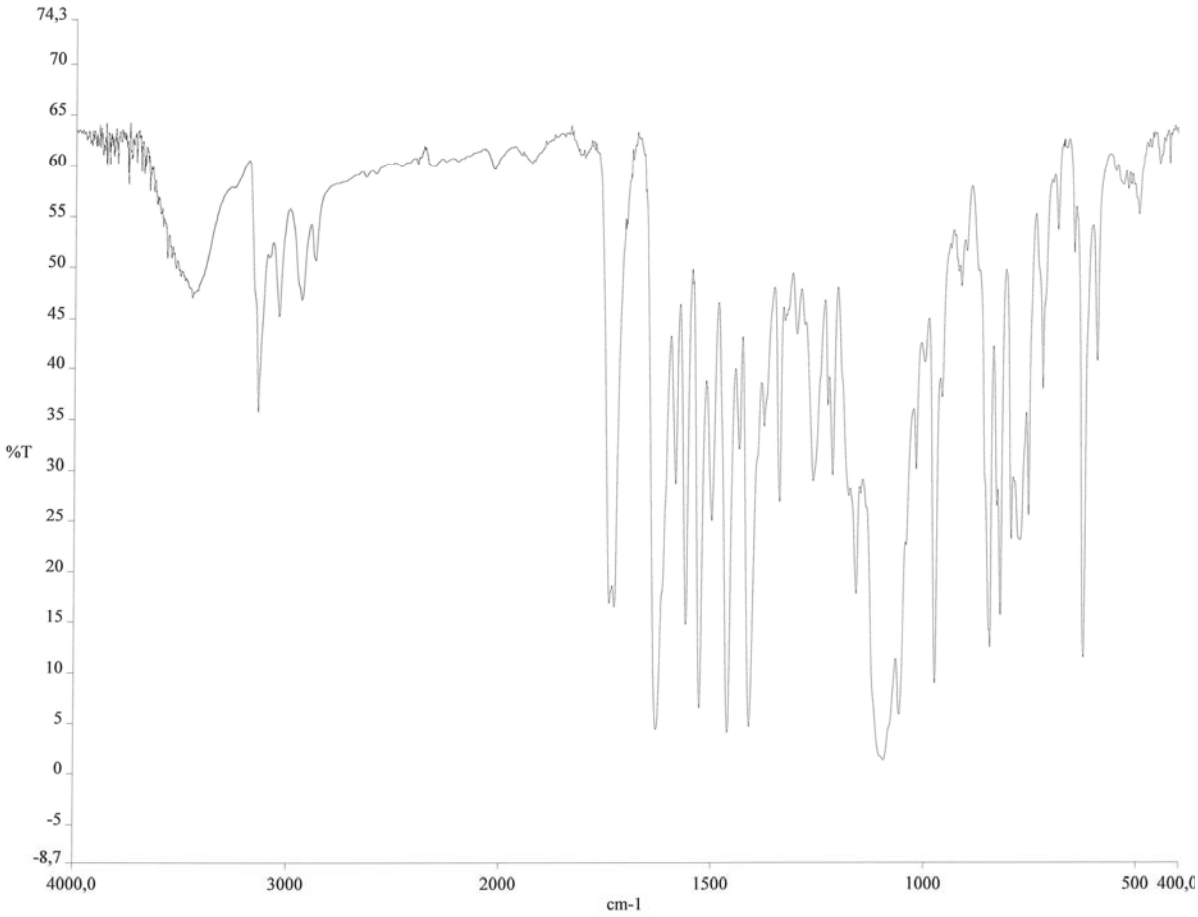

Figure S16. FT-IR spectrum of $[Fe(L2)_2](ClO_4)_2$ (**2**).

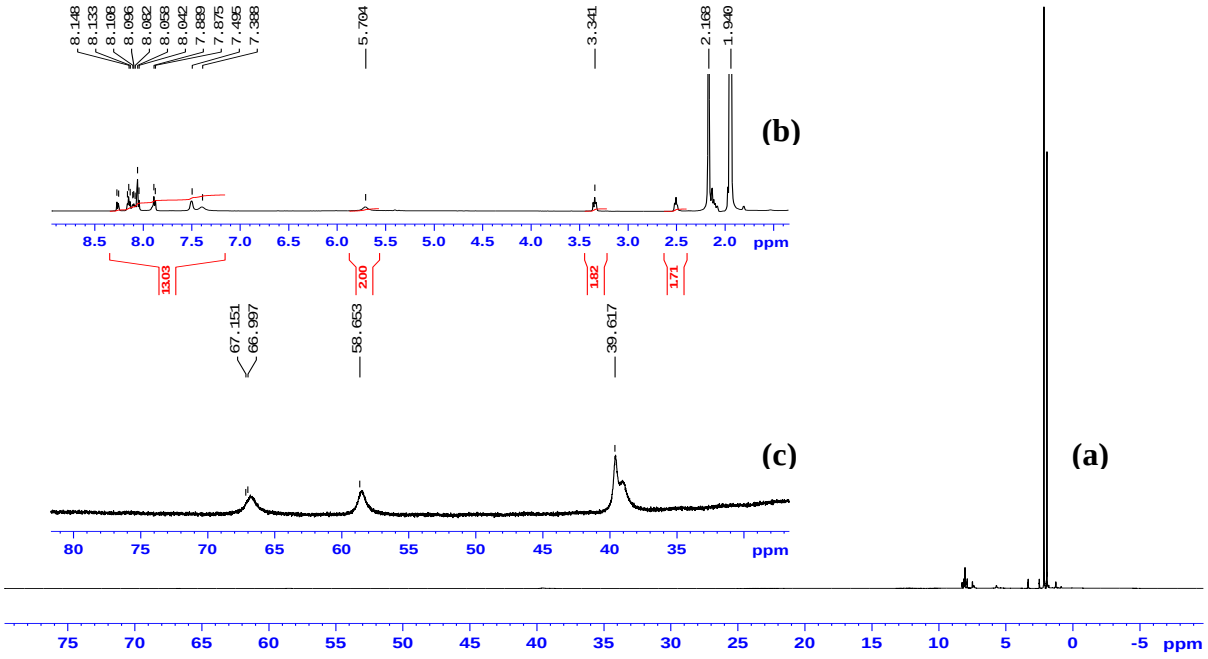

Figure S17. (**a**) ^{1}H NMR spectrum of $[Fe(L2)_2](BF_4)_2{\cdot}CH_3CN{\cdot}H_2O$ (**3**) in CD_3CN. Insets (**b**) and (**c**) show enlarged zones of the whole spectrum.

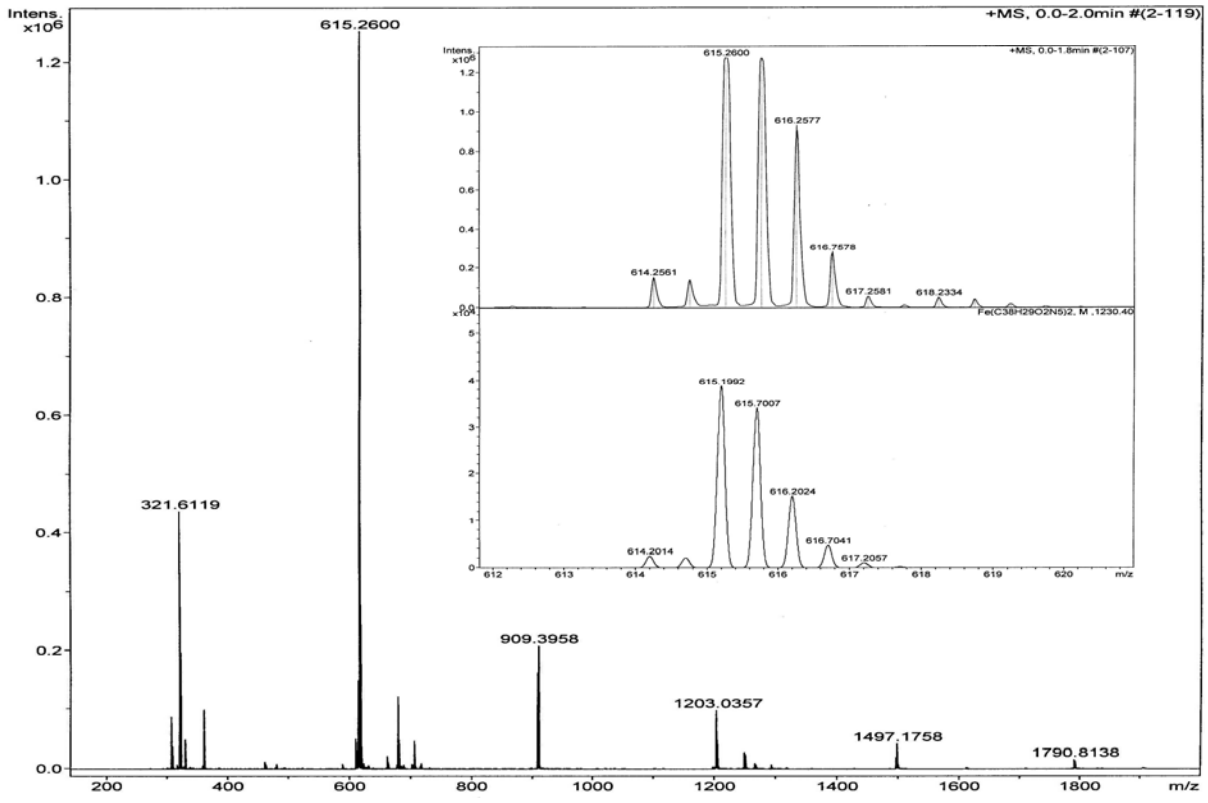

Figure S18. ESI-TOF spectrum of $[Fe(L2)_2](BF_4)_2{\cdot}CH_3CN{\cdot}H_2O$ (**3**). Experimental (up) and simulated (down) isotopic distributions for the most intense peak; $\mathbf{M}^{2+}$; are shown in the inset.

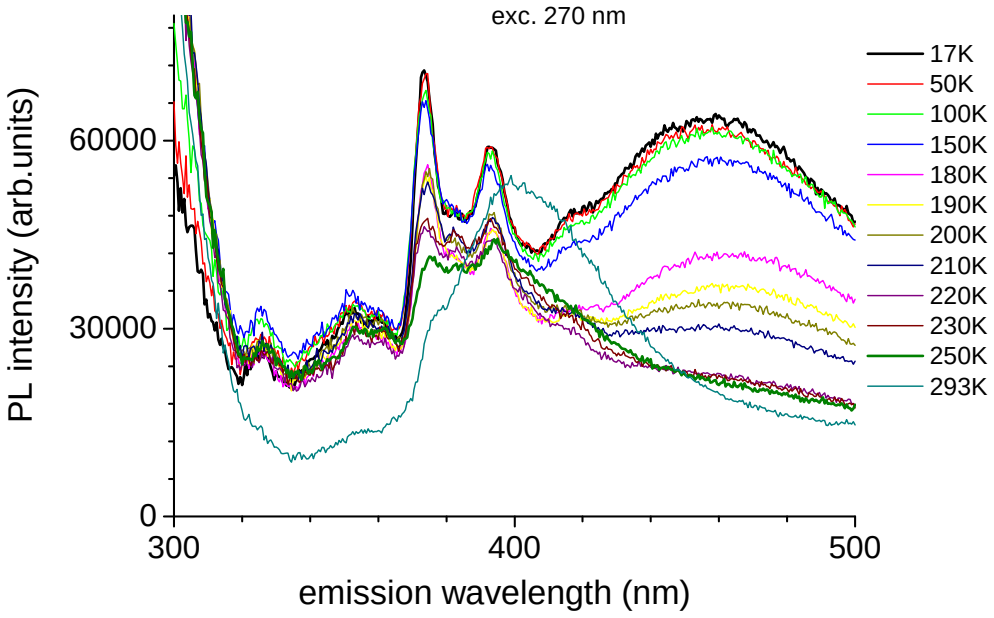

Figure S19. Emission spectra of compound **3** (polycrystalline) excited at 270 nm at different temperatures. The half-bandwidths of the excitation and emission monochromators corresponded to 4 nm

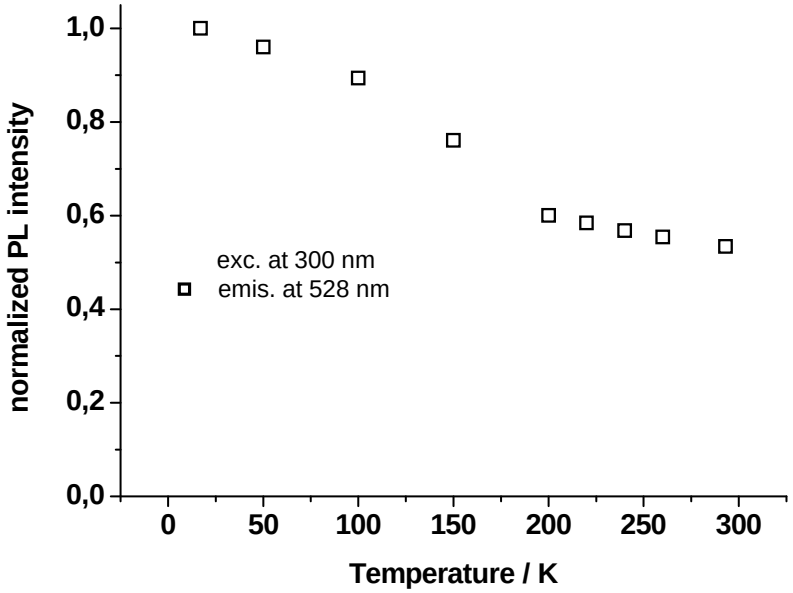

Figure S20. Normalized emission intensity of polycrystalline pyrene butyric acid as a function of the temperature. The excitation and emission wavelengths are 300 and 528 nm, respectively.